PCCP
REVIEW ARTICLE

Nanocrystallinity effects in lithium battery materials

Aspects of nano-ionics. Part IV

Janez Jamnik[ab] and Joachim Maier[a]

[a] *Max-Planck-Institut für Festkörperforschung, Heisenbergstraße 1, 70569, Stuttgart, Germany*
[b] *National Institute of Chemistry, Hajdrihova 19, SI-1000, Ljubljana, Slovenia*

Received 1st August 2003, Accepted 3rd October 2003
First published as an Advance Article on the web 28th October 2003

Nanostructured materials offer the possibility to make use of small transport lengths and small separation distances almost like in fluids, but unlike fluids, the higher structural stability of the solid state can be taken advantage of. Recent findings in the field of Li-batteries highlight the potential for room temperature applications. This paper addresses advantages and disadvantages of nanostructured matter with respect to stability, storage capacity, voltage and charging/discharging rates. In this context we discuss a novel interfacial storage mechanism for lithium which, in the mesoscopic case, forms a bridge between batteries and capacitors.

1. Introduction

It is well-known that electronic transport properties can be tuned by interfacial design and by varying the spacing of interfaces down to the nano-regime. For that reason, nano-electronics has become a well-established field in physics and materials science. Ionic transport properties are of similar significance (chemical kinetics of solids, electrochemical devices) for the physical chemistry of solids and for materials science, and essentially over the last two decades many experiments and theoretical considerations have shown the impact of interfaces and of the spacing of interfaces on ionic transport properties.[1] While fundamental aspects of nano-ionics have been addressed in previous papers (Part I–III,[2–4,5]), this contribution refers to the important field of Li-batteries. This application refers to low enough temperatures that provide sufficient stability of the metastable morphology which is inherent to nanocrystalline matter.

Owing to the strict thermodynamic and kinetic constraints with regard to the choice of materials for Li-ion batteries, it is highly desired to extend the palette of available candidates. The traditional ways in selecting appropriate materials are: (a) the choice of optimal bulk structures; and (b) the compositional optimisation by doping. Prominent examples of the first path are intercalation compounds such as TiS_2, $Li_{1-x}CoO_2$ or carbon offering beneficial storage capacities and Li-mobilities.[6–8] A recent example for the second path is the attempt to drastically increase the electronic conductivity of $LiFePO_4$[9] by doping with higher-valent metal ions. Similarly, as one tries to increase the ionic conductivity of solid electrolytes,[1] the electrode function can also be improved by interfacial engineering. In this respect, a novel research area emerges characterised by tailoring the electrode properties *via* introducing nanostructural features.[10–18] In comparison with the research on nanocrystalline solid electrolytes, the optimisation of electrode functions also has to envisage the storage capacity. Several recent examples are highly relevant in this context.

Poizot *et al.*[12] showed that a variety of transition metal oxides (*e.g.*, Co, Ni, Cu, Fe) can be used as anodes. They are reduced to the metal on Li incorporation. The result is a nanocomposite consisting of a metal and Li_2O. Surprisingly, this process is almost reversible in spite of poor reactivity and/or transport properties of massive Li_2O. This kind of storage mechanism has been found even for transition metal fluorides.[19] Interestingly, this reversibility has not been observed for some metal oxides MO (M = Sn, Sb, In, Pb, Zn) (see, *e.g.*, refs. 20 and 21). Unlike the transition metal oxides mentioned above, these metals form alloys with Li. It is not clear how far this is correlated with the kinetic issues. In cases of transition metal oxides or fluorides a sloped charge–discharge graph has been found in the voltage range in which the reaction to the metal has already been completed. The nanostructure is formed *in-situ* after the first cycles, thus needs not be prefabricated and stays constant or forms reversibly after the following cycles.

Padhi *et al.*[22] showed that $LiFePO_4$ can—in spite of its poor electronic conductivity—be used as a cathode material. Its efficiency can be much improved if, *e.g.*, a few nm thick carbon coating of individual $LiFePO_4$ particles formed *in-situ* during the $LiFePO_4$ synthesis is accomplished.[14] The carbon coating provides an efficient electronically conductive network for the poorly conducting phosphate particles (''nanopainting'') but it is still permeable enough for Li^+ ions. As far as the role of the size of the phosphate particles is concerned, there are different opinions in the literature.[15,24,25]

Also, interfacial contributions to the storage capacity have been reported: Beaulieu *et al.*[25] communicated Li storage in the grain boundaries of otherwise ''inactive'' $SnMn_3C$. Grugeon *et al.*[13] reported storage within the metastable organic coating formed on the redox active electrode.

In spite of interesting and advantageous effects observed in the nano-crystalline state, there are also drawbacks. One of the major difficulties stems from the fact that nano-crystallinity inherently introduces a perceptible excess energy and, thus, stability problems into the system (see section 2). The agglomeration of nanocrystalline Si during the performance of a Li/LiSi cell upon cycling as described in ref. 15 provides a relevant example. In order for Li-batteries to exhibit a stationary performance, the nanocrystalline materials have to rely on kinetic (rather than on thermodynamic) stability. For an

DOI: 10.1039/b309130a

elementary material (such as Li) this is an impossible task due to the high Li-mobility. In binary or multinary compounds, a high mobility of one constituent, *e.g.* Li, does not exclude morphological stability, as long as the other components are sufficiently immobile. In the case mentioned above, obviously, the mobility of Si which is sluggish when compared to Li is still too high to prevent the particle growth and agglomeration. Morphological stability can be further improved if several materials are combined in an appropriately structured composite.[26,27] Especially carbon coatings appeared to be efficient in this respect.[28]

In this paper, effects of the nanocrystalline state on the performance of Li-ion batteries are discussed from a rather conceptual point of view. As pointed out in ref. 29, two types of size effects may be distinguished: trivial size effects which rely solely on the increased surface-to-volume ratio, and true-size effects which also involve changes of local materials properties. After a brief discussion of thermodynamic aspects (cell voltage) size effects with respect to capacity, reaction kinetics and transport rates are considered. It is hoped that this discussion forms a frame within which different nano-crystallinity effects can be systematically addressed, and which may help to understand relevant phenomena.

2. Thermodynamic stability and emf

Before we start to discuss the kinetic issues it is certainly important to clarify how far equilibrium thermodynamics is affected, which will be reflected in modified phase stabilities and cell voltages.

The excess value of the grand thermodynamic potential of crystals with surfaces (tension γ_j, area a_j of plane j), edges (tension κ_k, length L_k of edge k) and corners (tension ε_l of corner l) is given by:[31] $\Omega^{\text{ex}} = \Sigma_j\gamma_j a_j + \Sigma_k\kappa_k L_k + \Sigma_l\varepsilon_l$. for the purpose of a first approximation we can neglect non-idealities such as point defects on the surface. If γ, κ and ε are assumed to be independent of size (which is usually fulfilled for sizes above 1 nm) and if the crystal is surrounded by a gas phase against which γ, κ and ε are measured, the equilibrium crystal shape is determined by[31]

$$\frac{1}{r_j}\left(\gamma_j + \sum\nolimits_k \kappa_k \frac{\partial L_k}{\partial a_j}\right) = \text{const}, \tag{1}$$

where r_j denotes the height of the crystal plane with respect to the origin. Ignoring edges and corners, the equilibrium shape adopts the Wulff form, *i. e.* $\gamma_j/r_j = \text{const}$,† for any surface j.

The excess chemical potential of the component α in a given Wulff-crystal is given by[33] $\mu_\alpha^{\text{ex}} = v_\alpha 2\bar{\gamma}/\bar{r}$, where $\bar{\gamma}$ and $\bar{r}$ are the area averaged γ- and r-values, *i. e.* $\bar{\gamma} \equiv \Sigma_j a_j\gamma_j/a$ and $\bar{r} = \Sigma_j a_j r_j/a$, while v_α denotes the partial molar volume of the component α. Even though the full equilibrium shape is usually not achieved, the above equations will be useful to estimate the energetic effects. According to the excess chemical potential, the Gibbs energy of reactions involving nanocrystalline matter of grain size $\bar{r}$ is modified and reads (ν_α: stoichiometry coefficient)

$$\Delta_{\text{R}} G = \Delta_{\text{R}} G(r \to \infty) + \sum\nolimits_\alpha 2\nu_\alpha \frac{\bar{\gamma}_\alpha}{\bar{r}_\alpha} v_\alpha. \tag{2}$$

The index α denotes the reaction partners and also the crystal to which the respective reaction partner refers. Let us consider an elemental crystal. The parameter v_α then becomes the molar crystal volume V_{m}. The surface tension $\bar{\gamma}$ of pure materials is typically of the order of 1 J m^{-2}. In realistic systems, the relevant γ-value is distinctly lower (interfacial tension of solid–liquid, solid–solid contacts). If we take a value of 0.1 J m^{-2} as a typical value for the materials under regard and further assume $v_\alpha = 25$ cm^3 mol^{-1} and $\bar{r} = 1$–100 nm as typical parameters, then μ^{ex} amounts to 0.1–10 kJ mo^{l-1}. This corresponds to an electrical voltage equivalent of 1–100 mV which might be perceived in the open circuit voltage, but is not of great significance for the overall electrical performance. Even though the Wulff-shape corresponds to a minimum free energy at given radius, it is not expected that other shapes lead to exceedingly higher values.

The above estimated values of the excess energy are much smaller than typical chemical reaction energies. Nevertheless, in special cases in which the competing G-values are not very different (*e.g.*, in phase transformations), the interfacial contribution may even be of qualitative influence. Thus, it has been suggested in ref. 34 that in nanocrystalline state anatase is thermodynamically stable while in the microcrystalline state rutile has the lowest free energy.

At smaller sizes, edge and corner effects become increasingly more important. As experience shows, they do not significantly change the overall energy unless we go below a size of typically a few nm. Then, however, we have to pay attention to the fact that structural changes come into play. At such extremely small sizes, it is better to use a bottom–up approach (by cluster calculations) than a top–down approach. The limit can in many cases be found to be on the order of 1 nm. To give an example: the rock salt structure of NaCl is found to be adopted for cluster sizes of 10 units ($\simeq$ 1 nm) and more, while below that value cluster chemistry dictates very different equilibrium structures.[35]

An important consequence of the nanocrystallinity is that we do no longer expect sharp plateaus in the charge–discharge curves‡ in the case of heterogeneous solid state reactions in multiphase regimes. Obviously, the $\bar{\gamma}/\bar{r}$ - term in the chemical potential offers one reason for this. Even though we do not have a homogeneous chemical potential for the immobile constituents, we can assume μ_{Li} to be spatially invariant and being given by[33]

$$\mu_{\text{Li}}(\bar{r}) = \mu_{\text{Li}}(\bar{r} \to \infty) + 2\frac{\bar{\gamma}(\bar{r})}{\bar{r}} v_{\text{Li}}. \tag{3}$$

If we consider a monomodal distribution, eqn. (3) indicates that $\mu_{\text{Li}}(\bar{r})$ and hence the cell voltage changes during the charging/discharging even in multiphase regimes whenever the grain size or the surface structure varies. This should be the rule rather than the exception. Eqn. (3) tells us also that at a given charge state a grain size distribution gives rise to a distribution in the Li-composition ($\nabla(\bar{\gamma}/\bar{r}) \neq 0$, hence $\nabla\mu_{\text{Li}}(\bar{r} \to \infty) \neq 0$, and thus $\nabla x_{\text{Li}} \neq 0$).

3. Reaction kinetics

In section 2 it was demonstrated that for typical nano-sized crystals the impact of surfaces on $\Delta_R G$ (eqn. (2)) may be perceptible, but usually not paramount. The reason lies in the fact that the bulk contribution prevails over the surface term simply due to the larger number of atoms sitting in the bulk. The situation in the case of reaction kinetics is fundamentally different. If the overall solid state reaction can be divided into the pure reaction step occurring on the surface (interface) and the accompanied transport steps occurring in bulk, then the kinetics of the reaction step is governed by the surface structure and hence strongly dependent on surface energetics. Owing to the effective curvature of small crystals, the density of edges, corners and the confined number of surface atoms becomes significant. Also, particular surface defects such as steps or surface vacancies are active owing to their increased local standard chemical potential. Thus, the activation energy

† At the contact to a neighbouring solid phase this expression has to be appropriately generalised, see ref. 32.

† We discuss here thermodynamic aspects, and hence stationary charge–discharge curves (*i.e.*, corresponding to very slow rates).

of the surface reaction will be strongly modified if compared to a surface reaction at a flat extended interface.

It is expected that the strongly modified surface reaction rate will have a strong impact on elementary processes during electrochemical deposition, nucleation, early growth and formation of the passivating layers. A further discussion requires information on details of the reaction mechanism which are not yet available.

4. Modified storage capacity of electrodes

The state-of-the-art storage mechanism in modern Li-batteries ("Li-ion batteries") occurs *via* insertion into the host electrode structure. As touched upon in the introduction, a high capacity can be achieved by storage that makes use of heterogeneous solid state reactions.[13,19] Both mechanisms are distinctly affected by grain size as far as kinetics (see next section) and surface thermodynamics are concerned. The specific storage capacity is not expected to be greatly altered. Besides this absorptive mechanism (insertion reaction) and this reactive mechanism (heterogeneous reaction) there is a third one, the adsorptive mechanism (reversible interfacial reaction), the capacity of which depends on the grain size in the first place and indeed resorts on the presence of nano-particles. Different possibilities of interfacial reactions have been mentioned in the literature: one is under-potential deposition[36] where typically a monolayer of Li is bonded on a metal associated with a partial charge transfer. A second possible mechanism is the lithium storage by reaction with the grain boundary phase[25] in polycrystalline materials or by reaction with the liquid electrolyte at the solid/liquid interface.[13,19] Here, we consider a third mechanism which has not been explicitly addressed in the field of Li-batteries, namely the charge separation at phase boundaries. Fig. 1 compares the homogeneous, absorptive storage (Fig. 1a) with this kind of storage that happens if the electrode particles exhibit only ionic conductivity (b) or if they exhibit only electronic conductivity (c). Then, only one charge constituent enters the particle (ions in case (b), *e.g.* in Li_2O, and electrons in case (c), *e.g.* in the case of a semiconductor. Obviously, if in the latter case we increase the electron density we approach the case of underpotential deposition). It is important to note that the same also happens on pure thermodynamic grounds, namely if the particle is completely saturated with respect to the neutral component it only accepts additional charge carriers on the account of interfacial charging (*i.e.* contact equilibrium in excess of phase equilibrium) before Li-deposition.

Naturally, the mechanism of interfacial storage will depend on the material. Let us consider the adsorptive storage of lithium characterised by electron injection (see Fig. 1c). In order to highlight the chemical driving force (reflected by the open circuit voltage) we simply consider a metal (*cf.* underpotential deposition) and distinguish between a metal M that cannot alloy with Li and a metal N that does. For the purpose of illustration we approximate the state shown in Fig. 1c in terms of a pure ionic bonding (full ionisation). Then, the contact situation is determined by the ionisation potential of Li, the electron affinity of M (or N) and a Coulomb term that measures the charge interaction. When we compare M with N and assess the energetics of the electron injection, it is essentially the electron affinity of the metal that is altered, the variation of which is also reflected in the variation of the electronegativity difference between metal and Li. While the electronegativity difference becomes very small if the metal can dissolve large quantities of Li, it remains large and offers a strong driving force in the case of the contact between Li and the metal M. Therefore, one expects interfacial charging preferentially in the case of a non-alloying metal. In fact, experiments provide indication for such a storage in the case of non-alloying transition metals.[19,38]

Let us now quantitatively discuss the size effect for the storage shown in Fig. 1b and without restriction of generality focus on the ion injection. For the calculation[38] we adopt a single step function for the standard chemical potential of electrons (Fig. 2). In addition, we set the step in μ°_{Li} to zero, since this only affects the open circuit situation. The situation resembles a usual double-layer capacitor with metal electrodes, the difference being that the space charge layer is formed within the interior rather than outside the electrode. The specific capacity of such an electrode is proportional to $1/L$, L being the particle size. Non-trivial nano-size effects are expected in the sub-Debye length regime in which the space charges overlap, *i.e.* for $L < \lambda$. We investigate this effect by exemplarily assuming the electrode to be shaped in the form of a thin layer (quasi one-dimensional system) (Fig. 2). For simplicity, we further assume Boltzmann statistics to apply. Fig. 3 shows the numerically calculated size dependence of the specific differential capacity for different electrode potentials. The solid lines refer to a situation in which the finite size of the ions[39] (*i.e.* Helmholtz-layer in liquid electrochemistry) was neglected. For thicknesses which are large compared to the Debye length, the specific capacity increases linearly with $1/L$, as expected. In the sub-Debye length regime, two interesting effects are observed: (i) the thickness dependence asymptotically disappears; and (ii) the value of the specific capacity approaches the value characteristic for the case of volume insertion (Fig. 3, dashed lines). In other words, in the sub-Debye regime there is almost no difference between the storage through volume insertion and storage through charge separation, at least as far as the capacity is concerned. The effect is less pronounced if the finite ion size (finite distance of the closest approach) is taken into account (Fig. 3, dotted plots). The critical L at which the difference between the two storage mechanisms disappears decreases with increasing space charge potential ψ and, thus, with the amount of Li inserted.

The storage *via* heterogeneous reaction, in principle, includes all storage modes discussed (Fig. 4). In the first stage (Fig. 4a) Li is homogeneously inserted into the bulk and

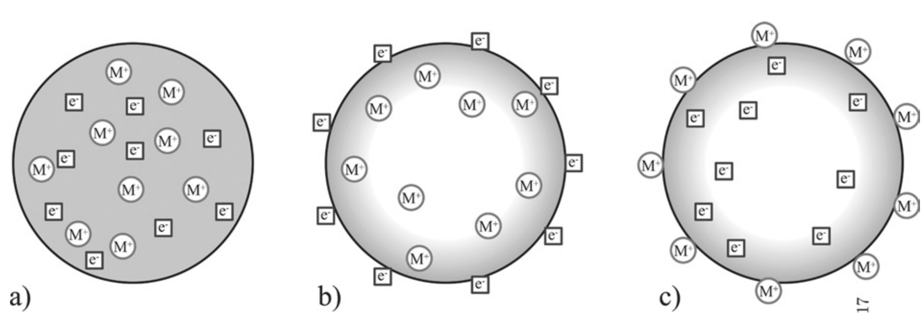

Fig. 1 Charge storage in electrode particles by means of (a) insertion reaction; (b), (c) interfacial reaction associated with charge separation. In case (b) solely ions, and in case (c) solely electrons are injected. Although in cases (b) and (c) no redox reaction takes place, the differential capacitance for very tiny samples could reach the values, as expected for a pure bulk insertion case (*cf.* Fig. 3).

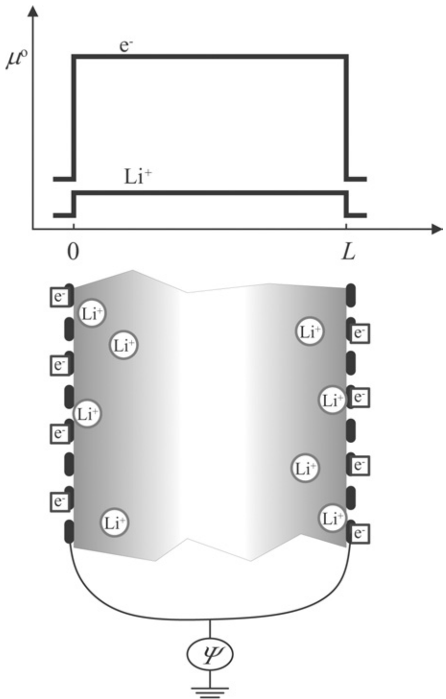

Fig. 2 Sketch of the cell considered in the calculation of space charge capacitance as a function of the size L. It consists of a pure Li^+ ion conductor sandwiched between two electronically conductive electrodes. The electrodes are at the potential ψ (*versus* Li metal) and permeable for Li^+ ions.

the charge/discharge curve $\mu_{Li}(x)$ exhibits the well-known characteristics of an insertion electrode (usually slightly sloped with additional possible anomalies due to structural transitions). After having reached the solubility limit (which depends also on the particle size, see section 2) new phases and hence

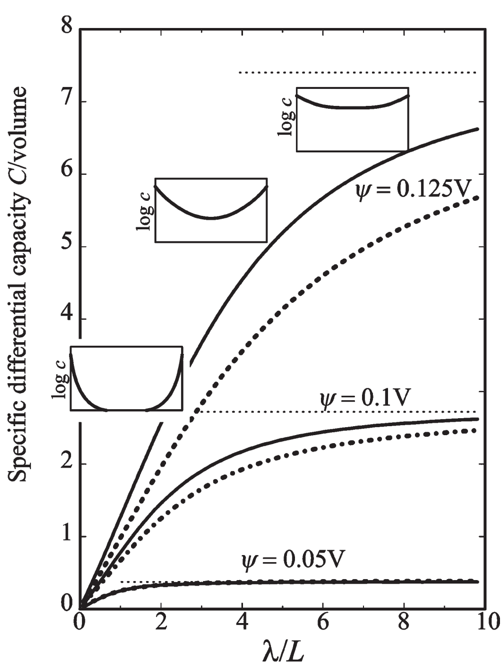

Fig. 3 Specific (per unit volume) differential capacity of the slab sketched on Fig. 2. Storage *via* charge separation is considered, the space charge potential ψ is normalised with respect to the thermal voltage, being the parameter. The difference between the solid and the dotted curves is due to the Helmholtz capacitance which was set to $0.1\varepsilon\varepsilon_0/\lambda$ in the case of dotted curves. For comparison, the capacitance values for the case in which homogeneous insertion would be possible are given (dashed lines).

interfaces are formed (Fig. 4b). The corresponding $\mu_{Li}(x)$ profile is expected to be nearly flat (non-vanishing slope due to nanocrystallinity effects, see section 2). Even if these phases no longer dissolve Li, further storage is possible *via* interfacial charging until $\mu_{Li}(x)$ becomes equal to the chemical potential of metallic lithium. As pointed out above, electron injection occurs at the surface of the non-alloying metal M while ion injection is probable at the Li_2O/M surface. Fig. 4c shows the expected charge carrier distribution if excess lithium is accommodated at the M/Li_2O interface which is likely to be formed in the course of the heterogeneous solid state reaction. In all these cases of interfacial storage $\mu_{Li}(x)$ resembles the characteristic of a capacitor. Such interfacial charging has been suggested to be very reversible unlike Li storage in the passivating layer that might also occur.[19]

5. Modified charging and discharging rates

The charging and discharging rates are determined by: (i) the transport through the electrolyte; (ii) the transport of Li^+ ions and electrons within the composite electrodes (usually *via* different pathways, *e.g.* ions along the pores occupied by liquid electrolyte, electrons along the surface of the electrochemically active particles and *via* carbon black particles) to the proper electrode particles; (iii) surface incorporation of Li^+ into the electrochemically active particles; and (iv) the transport within them accompanied with the electrochemical reaction. We will focus on steps (ii) and (iv), since they seem especially interesting in this context.

Transport of Li^+ ions and electrons to the electrode particles

The distribution topology of fast electronic and ionic pathways within the electrode decisively determines the kinetics of the subsequent steps (iii) and (iv). Whilst a simple random mixture of, *e.g.*, $LiFePO_4$ and carbon black (the fraction of the latter being above the percolation threshold) provides good electronic conductivity of the overall material, it however offers quite poor charging properties. If, however, the topology of fast electronic and ionic pathways is such that all the particles are effectively wired in parallel, much faster charging and discharging rates are achieved.

Besides using carbon, fast ionic and electronic interconnecting pathways within the composite could also be provided by enhanced surface conductivity of the electrochemically active particles themselves. There are many examples of enhanced surface conductivities due to space charge layers in composite and polycrystalline ionic and electronic conductors.[1] The space charge layers within the particles in composite electrodes do not form only upon charging/discharging in the case of the heterogeneous insertion (Fig. 1b) but, in general, at each interface in thermodynamic equilibrium. Fig. 5 displays exemplarily how the space charge conductance of an effectively one-dimensional system depends on the particle size (please note the similarity with the capacity behaviour shown in Fig. 3). In the case shown in Fig. 5 it is assumed that the surface concentration c_0 ($\gg c_\infty$) of the relevant charge carrier is approximately constant and that its mobility u is size independent. The two horizontal lines denote two important values: (i) mean specific space charge conductivity of the semi-infinite case, $qu\sqrt{c_0 c_\infty}$ (q denotes the charge carried per carrier); and (ii) the limiting value which is calculated assuming that the whole sample adopts the surface concentration c_0. The excess of the real conductivity values with respect to the first line,[41] $g(L)$, reflects the local size dependent changes of concentration, referring to a true size effect. In the field of lithium batteries, these effects have hardly been studied.

Certainly, the situation here is much more demanding, not only due to complex microstructure but also due to

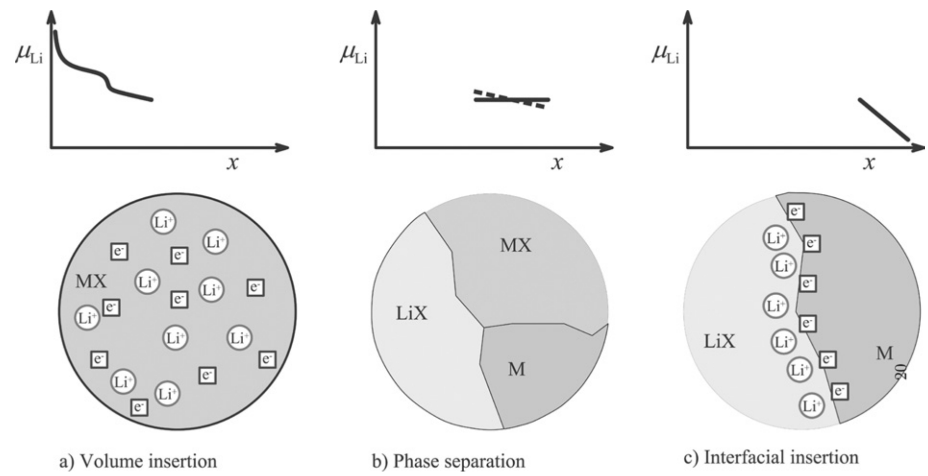

Fig. 4 Sequence of three different stages of a Li storage. Insertion in the bulk of MX (a). If the solubility limit is exceeded a heterogeneous solid state reaction characterised by phase separation occurs (b). Finally, the interfacial charging takes place (c).

compositional and structural variations upon charging and discharging. The experimental fact that the electronic conductivity of dry $LiMn_2O_4$ is far less than the conductivity of the same material when built and cycled in a Li-ion battery[41] may be correlated with such effects.

Transport within the electrode particles

The size dependence of rates referring to step (iv) depends on the storage mechanisms considered. If we discuss, *e.g.*, an insertion cathode material, then the over-potential due to step (iv) will be inversely proportional to the sum of ionic, R_{ion}, and electronic, R_{eon}, particle resistances (see, *e.g.*, ref. 42). If the conductivities, σ_{ion} and σ_{eon}, can be considered as position independent, R_{ion} and R_{eon} will be proportional to L^{-1}; assuming that all the particles are wired in parallel and are in contact with the electrolyte, the polarisation resistance per mass unit will decrease with L^2. Due to different technologies used in the preparation of electrode materials the topology of particle wiring certainly differs. We think that this is one of the main reasons for different findings[14,23] with regard to the importance of particle size for charging and discharging rates.

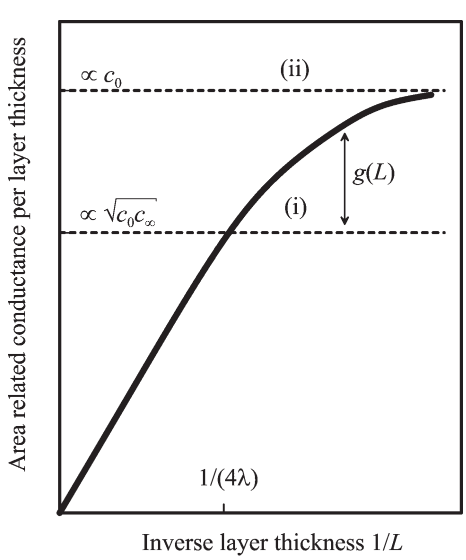

Fig. 5 Effective conductivity of a slab in lateral direction. The dashed lines denote two characteristic values: (i) the effective conductivity of non-overlapping space charge zones (assuming the effective thickness of the zones to be 2λ); and (ii) the conductivity as in the case of spatially homogeneous concentration c_0.

As discussed above, even rather poor mixed conductivity does not prevent materials from being considered for homogeneous Li-insertion, if proper wiring is achieved. If, however, a material is a pure ionic or a pure electronic conductor ambipolar diffusion will be too sluggish for practical relevance. Nevertheless, this does not prevent the use of such a material for interfacial charging (Fig. 1b). In such a case only ionic or only electronic conductivity (not both) need to be sufficiently high. The transport rates achieved are determined by the self diffusion coefficient (not chemical diffusion coefficient) of the mobile charge carrier solely and by the distance over which the charge separation takes place (usually equal or less than Debye length). For very small particles the capacity approaches that of the insertion mechanism, while for larger particles the increased storage speed may still offer benefits.

Finally, we will make a brief statement with respect to electronic properties. If they are polaronic in nature, the size effect on the transport properties should be similar to those of ionic defects. If we deal with delocalised states, quantum confinement effects come into play at much larger sizes and also tunneling effects may assist in contact and percolation problems addressed.

In short, the nanocrystallinity state may be very beneficial for the room temperature applications such as Li-batteries since, in a certain way it forms the bridge between the completely homogeneous fluid state and the structurally stable solid state.

Acknowledgements

Many useful discussions with Dr Miran Gaberscek and Dr Hong Li are gratefully acknowledged.

References

1 J. Maier, *Prog. Solid State Chem.*, 1995, **23**, 171–263.
2 J. Maier, *Solid State Ionics*, 2002, **154–155**, 291–201.
3 J. Maier, *Solid State Ionics*, 2003, **157**, 327–334.
4 J. Maier, *Solid State Ionics*, 2002, **148**(3,4), 367–374.
5 J. Maier, *Z. Phys. Chem.*, 2003, **217**, 415–436.
6 M. S. Whittingham, *Science (Washington, D. C.)*, 1976, **192**, 1126–1127.
7 K. Mitzushima, P. C. Jones, P. J. Wiseman and J. B. Goodenough, *Mater. Res. Bull.*, 1980, **15**, 783–789.
8 K. Ozawa, *Solid State Ionics*, 1994, **69**, 212–221.
9 S.-Y. Chung, J. T. Bloking and Y.-M. Chiang, *Nature Mater.*, 2002, **2**, 123–128.
10 J.-M. Tarascon and M. Armand, *Nature (London)*, 2001, **414**, 359–367.

11 L. F. Nazar, G. Goward, F. Leroux, M. Duncan, H. Huang, T. Kerr and J. Gaubicher, *Int. J. Inorg. Mater.*, 2001, **3**, 191–200.
12 P. Poizot, S. Laruelle, S. Grugeon, L. Dupont and J.-M. Tarascon, *Nature (London)*, 2000, **407**, 496–499.
13 S. Grugeon, S. Laruelle, R. Herrera-Urbina, L. Dupont, P. Poizot and J. M. Tarascon, *J. Electrochem. Soc.*, 2001, **148**, A285–A292.
14 N. Ravet, J. B. Goodenough, S. Besner, M. Simoneau, P. Hovington and M. Armand, Abstract 127, The 1999 Joint International Meeting Abstracts, Honolulu, HI, Oct. 17–22, 1999.
15 H. Li, X. J. Huang, L. Q. Chen, G. W. Zhou, Z. Zhang, D. P. Yu, Y. J. Mo and N. Pei, *Solid State Ionics*, 2000, **135–137**, 181–191.
16 S. H. Kang, J. B. Goodenough and L. K. Rabenberg, *Electrochem. Solid St. Lett.*, 2001, **4**, A49–A51.
17 J. Schoonman, *Solid State Ionics*, 2000, **135**, 5–19.
18 L. Kavan, M. Graetzel, J. Rathousky and A. Zukal, *J. Electrochem. Soc.*, 1996, **143**, 394–400.
19 H. Li, G. Richter and J. Maier, *Adv. Mater.*, 2002, **15**, 735–739.
20 I. A. Courtney and J. R. Dahn, *J. Electrochem. Soc.*, 1997, **144**, 2045–2052.
21 H. Li and L. Chen, *Solid State Ionics*, 1999, **123**, 189–197.
22 A. K. Padhi, K. S. Nanjundaswararny and J. B. Goodenough, *J. Electrochem. Soc.*, 1997, **144**, 1188.
23 H. Huang, S.-C. Yin and L. F. Nazar, *Electrochem. Solid State Lett.*, 2001, **4**, A170–A172.
24 Z. H. Chen and J. R. Dahn, *J. Electrochem. Soc.*, 2002, **149**, A1184–A1189.
25 L. Y. Beaulieu, D. Larcher, R. A. Dunlap and J. R. Dahn, *J. Electrochem. Soc.*, 2000, **147**, 3206–3212.
26 Y. Idota, T. Kubota, A. Matsufuji, Y. Maekawa and T. Miyasaka, *Science (Washington, D. C.)*, 1997, **276**, 1395–1397.
27 H. Li, Q. Wang, L. H. Shi, L. Q. Chen and X. J. Huang, *Chem. Mater.*, 2002, **14**, 103–108.
28 M. Yoshio, H. Y. Wang, K. Fukuda, T. Umeno, N. Dimov and Z. Ogumi, *J. Electrochem. Soc.*, 2002, **149**, A1598–A1603.
29 J. Maier, *Solid State Ionics*, 2002, **154–155**, 291–301.
30 A. I. Rusanov, *Phasengleichgewichte und Grenzflächenerscheinungen*, Akademie-Verlag, Berlin, 1978, in German.
31 C. Herring, *J. Appl. Phys.*, 1950, **21**, 437–445.
32 R. Kaischew, *Bull. Acad. Bulg. Sci. Phys.*, 1950, **1**, 100.
33 R. Defay, I. Prigogine, A. Bellemans and H. Everett, *Surface Tension and Adsorption*, Wiley, New York, 1960.
34 H. Z. Zhang and J. F. Banfield, *Am. Mineral.*, 1999, **84**, 528–535; A. A. Gribb and J. F. Banfield, *Am. Mineral.*, 1997, **82**, 717–728.
35 T. P. Martin, Festkörperprobleme (Advances in Solid State Physics), vol. XXIV, Vieweg, Braunschweig, 1984, 1, in German.
36 B. E. Conway, *Electrochim. Acta*, 1993, **38**, 1249–1258.
37 P. Balaya, H. Li, L. Kienle and J. Maier, *Adv. Funct. Mater*, 2003, **13**, 621–625.
38 J. Jamnik, J. Maier and S. Pejovnik, *Solid State Ionics*, 1995, **75**, 51–58.
39 J. R. Macdonald, D. R. Franceschetti and A. P. Lehnen, *J. Chem. Phys.*, 1980, **73**, 5272–5293.
40 J. Maier, *Solid State Ionics*, 1987, **23**, 59–67.
41 J. Molenda, K. Swierczek, M. Molenda and J. Marzec, *Solid State Ionics*, 2000, **135**, 53–59.
42 J. Jamnik, *Solid State Ionics*, 2003, **157**, 19–28.